Forced Oscillations with Nonlinear Restoring Force

By

Chihiro HAYASHI

Department of Electrical Engineering

(Received July, 1951)

Abstract

Forced oscillations with nonlinear restoring force are studied in transient states as well as in steady states. The differential equations which govern the oscillations are under some restrictions transformed to the form:

$$dy/dx = Y(x,y)/X(x,y),$$

and the integral curves of this equation are studied according to Poincaré and Bendixson with the basic idea that the singularities of the above equation are correlated with the periodic steady states of oscillation and the integral curves with transient states.

With this method of investigation we have first studied the harmonic oscillations in Part I, then the subharmonic oscillations in Part II. In both cases the theoretical analyses are compared with experimental results, and the satisfactory agreement is found between them.

Introduction

A differential equation

$$\frac{d^2v}{d\tau^2} + k\frac{dv}{d\tau} + f(v) = B\cos\tau, \tag{1.1}$$

in which $f(v)$ is nonlinear, occurs in several different kinds of physical problems. As will be shown later, the case of alternating current circuits containing iron core inductances is an example which leads to Eq. (1.1).

From the theory of differential equations, it is known that Eq. (1.1) possesses solutions $v(\tau)$ which are uniquely determined once the values of $v(0)$ and $(dv/d\tau)_{\tau=0}$, the initial conditions, are prescribed. In case of linear oscillations where $f(v)$ in Eq. (1.1) is proportional to v, there is one and only one periodic solution after some transients have died out. It is, however, the distinctive character of nonlinear oscillations that the various types of periodic solutions of Eq. (1.1) may exist

corresponding to the different values of the initial conditions given.

In the following lines we concentrate our attention to the stability of periodic solutions and, in particular, to the transient states of oscillations which give rise to the periodic steady states according to the initial conditions prescribed.

Part I. Harmonic Oscillations

1. Periodic Solutions and their Stability

We shall first deal with the harmonic oscillations i. e., the periodic solutions $v(\tau)$ of Eq. (1. 1) in which the period is the same as the period 2π of the external force $B\cos\tau$. Afterwards subharmonic oscillations, in which the solution $v(\tau)$ has as its least period an integral multiple (different from unity) of the period of the external force, will be treated in Part II.

Very little generality is lost by choosing for the restoring force $f(v)$ in Eq. (1. 1) the following cubic in v:

$$f(v) = v^3, \tag{1.2}$$

so that Eq. (1. 1) becomes

$$\frac{d^2v}{d\tau^2} + k\frac{dv}{d\tau} + v^3 = B\cos\tau\,. \tag{1.3}$$

For the harmonic oscillations in which the oscillation of the fundamental frequency predominates over the higher harmonics, Eq. (1. 3) admits a solution of the form:

$$v(\tau) = x(\tau)\sin\tau + y(\tau)\cos\tau\,. \tag{1.4}$$

The amplitudes $x(\tau)$, $y(\tau)$ are the functions of τ and are reduced to constants after the transient states have elapsed. Substituting Eq. (1. 4) into Eq. (1. 3) and separately equating the terms containing $\sin\tau$ and $\cos\tau$ to zero, we obtain

$$\left.\begin{aligned} \frac{dx}{d\tau} &= \frac{1}{2}\left[B - kx + y - \frac{3}{4}r^2y\right] \equiv X(x, y), \\ \frac{dy}{d\tau} &= \frac{1}{2}\left[-x - ky + \frac{3}{4}r^2x\right] \equiv Y(x, y), \\ \text{where} \quad & \\ r^2 &= x^2 + y^2\,. \end{aligned}\right\} \tag{1.5}$$

We have, however, to set down the following restrictions for the derivation of Eqs. (1. 5), i. e.,

1. The amplitudes $x(\tau)$, $y(\tau)$ are functions of τ but only slowly variable, viz.,

$$dx/d\tau \ll x\ , \qquad dy/d\tau \ll y\ ,$$
$$d^2x/d\tau^2 \ll dx/d\tau\ , \quad d^2y/d\tau^2 \ll dy/d\tau\ ,$$

so that $d^2x/d\tau^2$ and $d^2y/d\tau^2$ may be neglected.

2. The damping coefficient k is a relatively small quantity.

The results derived from Eqs. (1.5) are therefore not applicable to the case in which the higher harmonic oscillations are sustained. Whereas in our present study, Eqs. (1.5) may be assumed to be legitimate as far as we deal with the harmonic oscillations.

In the steady states, where the amplitudes $x(\tau)$, $y(\tau)$ of Eq. (1.4) are constant,

$$\left.\begin{aligned} dx/d\tau &= X(x,\ y) = 0\ , \\ dy/d\tau &= Y(x,\ y) = 0\ . \end{aligned}\right\} \tag{1.6}$$

From Eqs. (1.5) and (1.6), the amplitude r_0 of the periodic solution $v(\tau)$ is given by

where
$$\left.\begin{aligned} B^2 &= r_0^2(A^2+k^2)\ , \\ A &= \frac{3}{4}r_0^2-1\ , \end{aligned}\right\} \tag{1.7}$$

and the components x_0, y_0 of r_0 are found as:

or
$$\left.\begin{aligned} &Bx_0 = kr_0^2\ , \quad Ax_0 = ky_0\ , \\ &x_0^2 = \frac{r_0^2}{1+\left(\frac{A}{k}\right)^2}\ , \quad y_0^2 = \frac{r_0^2}{1+\left(\frac{k}{A}\right)^2}\ . \end{aligned}\right\} \tag{1.8}$$

The circumstances under which this condition obtains are determined by a further stability investigation. To effect this we shall consider small variations ξ and η from the solution x_0 and y_0 as obtained from Eqs. (1.8), and determine whether these deviations approach zero or not with the time τ.

From Eqs. (1.5) we have

$$\left.\begin{aligned} \frac{d\xi}{d\tau} &= \frac{\partial X}{\partial x}\xi + \frac{\partial X}{\partial y}\eta\ , \\ \frac{d\eta}{d\tau} &= \frac{\partial Y}{\partial x}\xi + \frac{\partial Y}{\partial y}\eta\ . \end{aligned}\right\} \tag{1.9}$$

The solutions of these simultaneous equations have the form $e^{\lambda\tau}$, and λ is determined by

$$\begin{vmatrix} \frac{\partial X}{\partial x}-\lambda & \frac{\partial X}{\partial y} \\ \frac{\partial Y}{\partial x} & \frac{\partial Y}{\partial y}-\lambda \end{vmatrix}=0. \tag{1.10}$$

The variations ξ and η approach zero with the time τ, provided that the real part of λ is negative, and the corresponding periodic solutions determined from Eqs. (1.4) and (1.8) are stable. This stability condition[1] is given by Hurwitz's criterion[2] as:

$$\left.\begin{aligned} &-\frac{\partial X}{\partial x}-\frac{\partial Y}{\partial y}>0, \\ \text{and}\quad &\\ &\frac{\partial X}{\partial x}\frac{\partial Y}{\partial y}-\frac{\partial Y}{\partial x}\frac{\partial X}{\partial y}>0. \end{aligned}\right\} \tag{1.11}$$

Substituting Eqs. (1.5) and (1.7) into Eqs. (1.11), we obtain

$$\left.\begin{aligned} &k>0, \\ \text{and}\quad &\\ &\frac{27}{16}r_0^4-3r_0^2+k^2+1>0 \quad \text{or} \quad \frac{dB^2}{dr_0^2}>0. \end{aligned}\right\} \tag{1.12}$$

Evidently the first condition holds since we are concerned with the positive damping. The second condition shows that the periodic solution is stable under such circumstances that the amplitude r_0 increases with increasing external force B. This is quite a plausible condition.

2. Analysis of the Nonlinear Oscillations by means of Integral Curves

As we have already mentioned, our object is, in particular, to study the transient solutions of Eq. (1.3), which yield to the periodic solutions with the lapse of time τ. For this purpose it is useful to investigate following Poincaré[3] and Bendixson[4] the integral curves of the following equation derived from Eqs. (1.5), i.e.,

$$\frac{dy}{dx}=\frac{Y(x,\ y)}{X(x,\ y)}. \tag{2.1}$$

Since the time τ does not occur explicitly in Eq. (2.1), we can draw the integral curves in the x, y-plane with the aid of the isocline method or otherwise.[5] As

1) This condition may fail if the higher harmonic oscillations are predominantly superposed on the harmonic oscillation with negative damping. A more rigorous criterion for the stability will be given in a later paper.

2) A. Hurwitz, Math. Ann., vol. 46, p. 273 1895).

3) H. Poincaré, Oeuvres, vol. 1, Gauthier-Villars, Paris, 1928, pp. 1-222.

4) I. Bendixson, Acta Mathematica, vol. 24, pp. 1-88 1901.

5) Another form of graphical solution has been given by A. Liénard, Rev. Gén. de l'Élec., vol. 23, pp. 901, 946 (1928).

mentioned in the preceding section, periodic solutions are correlated with $x(\tau)=$ constant, $y(\tau)=$constant of Eqs. (1.5) and hence with the singular points of Eq. (2.1), i.e., the points at which $X(x, y)$ and $Y(x, y)$ vanish simultaneously.

Now, suppose we fix a point $x(0)$, $y(0)$ in the x, y-plane as the initial condition, then the point $x(\tau)$, $y(\tau)$ moves, with the lapse of time τ, on the integral curve which pass through the point $x(0)$, $y(0)$, and gets finally to the stable singular point.[6] Hence the transient solutions are correlated with the integral curves of Eq. (2.1) and the time variation of $v(\tau)$ is obtained by the following line integral derived from Eqs. (1.5) as:

$$\tau=\int\frac{ds}{\sqrt{X^2(x, y)+Y^2(x, y)}}, \quad ds=\sqrt{(dx)^2+(dy)^2}, \tag{2.2}$$

where ds is the line element on the integral curve.

We turn, for a time, to a discussion of the character of the integral curves in the neighborhood of the singular points of Eq. (2.1). For the singular points, the roots of the characteristic equation (1.10) are given by Eqs. (1.5) as:

$$\left.\begin{aligned}
&\lambda_{1,2}=\frac{a_1+b_2\pm\sqrt{(a_1-b_2)^2+4a_2b_1}}{2},\\
&\text{with}\\
&a_1=\left(\frac{\partial X}{\partial x}\right)_{\substack{x=x_0,\\ y=y_0}}=\frac{1}{2}\left[-k-\frac{3}{2}x_0y_0\right],\\
&a_2=\left(\frac{\partial X}{\partial y}\right)_{\substack{x=x_0,\\ y=y_0}}=\frac{1}{2}\left[1-\frac{3}{4}\left(x_0^2+3y_0^2\right)\right],\\
&b_1=\left(\frac{\partial Y}{\partial x}\right)_{\substack{x=x_0,\\ y=y_0}}=\frac{1}{2}\left[-1+\frac{3}{4}\left(3x_0^2+y_0^2\right)\right],\\
&b_2=\left(\frac{\partial Y}{\partial y}\right)_{\substack{x=x_0,\\ y=y_0}}=\frac{1}{2}\left[-k+\frac{3}{2}x_0y_0\right].
\end{aligned}\right\} \tag{2.3}$$

It has been introduced by Poincaré[7] that the types of singular points are classified according to circumstances of the integral curves near the singular points, viz., according to the nature of the characteristic roots λ, as follows:

1. The singularity is a nodal point, in case the characteristic roots are real numbers with same sign, i.e.,

$$\left.\begin{aligned}
&(a_1-b_2)^2+4a_2b_1\geqq 0,\\
&a_1b_2-a_2b_1>0.
\end{aligned}\right\} \tag{2.4}$$

6) According to Bendixson (loc. cit., p. 73), it will be verified without difficulty that the integral curves of Eq. (2.1) have no limit cycle provided that the original differential equation is referred to the form of Eq. (1.1).

7) Loc. cit,. p. 14.

2. The singularity is a saddle point, in case the two roots are real numbers with opposite signs, i. e.,

$$\left.\begin{aligned}&(a_1-b_2)^2+4a_2b_1>0\,,\\&a_1b_2-a_2b_1<0\,.\end{aligned}\right\}\tag{2.5}$$

3. The singularity is a spiral point, in case the two roots are conjugate complex to each other, i. e.,

$$(a_1-b_2)^2+4a_2b_1<0\,.\tag{2.6}$$

In particular, if the two roots are pure imaginary, i. e., $a_1+b_2=0$, the singularity is either a center or a spiral.[8]

We also refer to a singularity as stable or unstable according to whether a point on any integral curve moves into the singularity or not with increasing τ, i. e., according to whether the real part of λ is negative or positive.

Following to the preceding considerations, we turn now to the present case of harmonic oscillations. Equations (1.7) furnishes in Fig. 1 the relation between B and r_0^2 for several values of k.

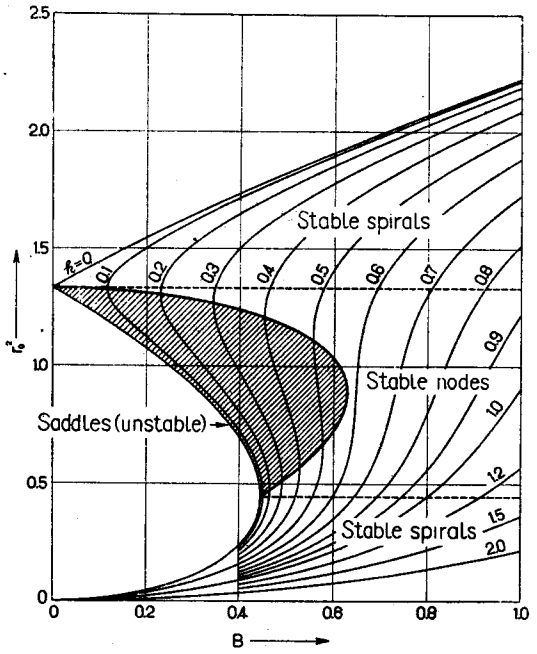

Fig. 1. Response curves and the correlated singularities for the harmonic oscillations.

By means of the foregoing analysis, we shall classify these periodic states of equilibrium[9] according to the types of the singularities. The boundary line between nodes and saddles is determined by Eqs. (2.4) and (2.5) as:

$$a_1b_2-a_2b_1=0\,,$$

or substituting Eqs. (2.3), we obtain

8) Poincaré loc. cit., p. 95) has shown the rigorous criterion to distinguish between a center and a spiral in case when $(a_1-b_2)^2+4a_2b_1<0$ and $a_1+b_2=0$.

9) These periodic states of equilibrium are not necessarily sustained, and they are only able to last out so long as they are correlated with the stable singularities.

$$\frac{27}{16}r_0^4 - 3r_0^2 + k^2 + 1 = 0\,. \tag{2.7}$$

This equation is identical with $dB^2/dr_0^2=0$ [cf. Eq. (1.12)], and the region of the saddle points is represented with shades where dB^2/dr_0^2 is negative. Since one root of λ is always positive, the periodic states in this region are unstable. This agrees with the result obtained in the preceding section.

Similarly, the boundary lines between nodes and spirals are determined by Eqs. (2.4) and (2.6) as:

$$(a_1 - b_2)^2 + 4a_2b_1 = 0\,,$$

or substituting Eqs. (2.3), we obtain

$$\frac{27}{16}r_0^4 - 3r_0^2 + 1 = 0\,, \quad \text{i.e.,} \quad r_0^2 = \frac{4}{3}\,,\ \frac{4}{9}\,. \tag{2.8}$$

These boundaries are drawn with dotted lines in Fig. 1. Since $a_1+b_2=-k$ by Eqs. (2.3), it is readily seen that the periodic states of equilibrium in the regions of nodes and spirals are evidently stable.

3. Geometrical Discussion of Integral Curves in Special Cases

In the preceding section we have briefly referred to the transient solutions which are correlated with the integral curves of Eq. (2.1). It is, however, useful and illuminating to consider the integral curves for some typical cases. The special cases we have in mind are

1. $k = 0.2\,,\quad B = 0.3\,,$

and

2. $k = 0.7\,,\quad B = 0.75$

in Eq. (1.3). As observed in Fig. 1, there are three different states of equilibrium in the first case 1, whereas we have only one periodic solution in the second case 2. The integral curves for these two cases are shown in Figs. 2 and 3 respectively. The singularities are determined by Eqs. (1.6) and summed up in the following table.

singular point	x_0	y_0	$\lambda_{1,2}$	classification
Figure 2, (1)	0.067	−0.310	$-0.100 \pm 0.423i$	stable spiral
ditto, (2)	0.699	−0.748	0.170, −0.370	saddle (unstable)
ditto, (3)	1.012	0.702	$-0.100 \pm 0.289i$	stable spiral
Figure 3	0.983	−0.295	−0.082, −0.618	stable node

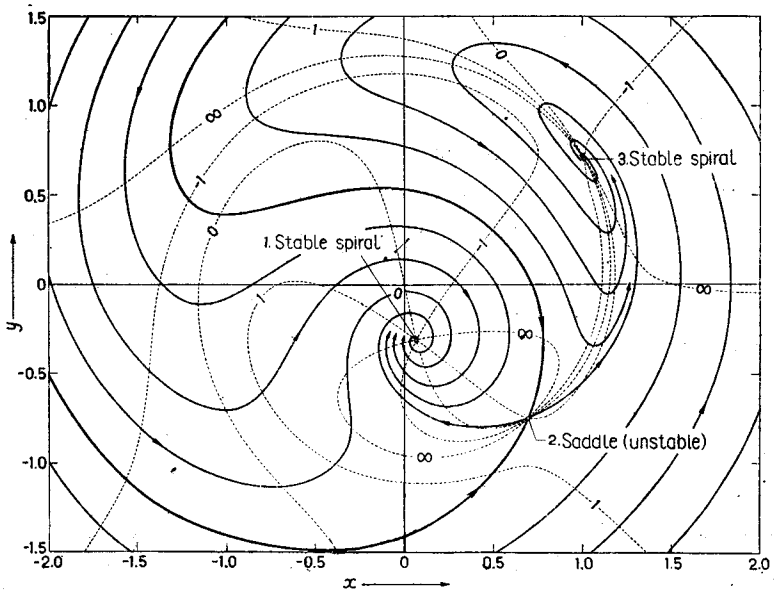

Full lines: integral curves Dotted lines: isoclines

Fig. 2. Integral curves for the harmonic oscillations with three singularities.

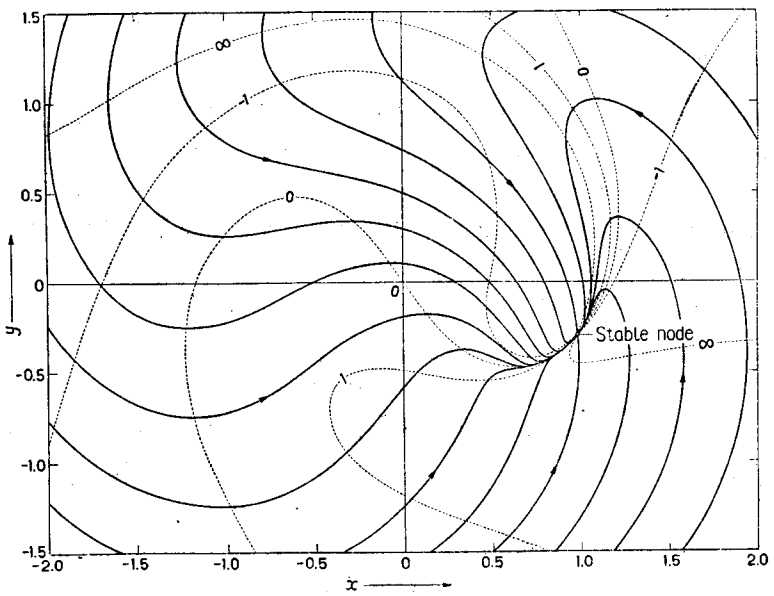

Full lines: integral curves Dotted lines: isoclines

Fig. 3. Integral curves for the harmonic oscillation with one singularity.

The integral curves are drawn with the aid of the isoclines represented by dotted lines, on which the numerics show the values of dy/dx for the respective isoclines. By Eqs. (1.5), a point $x(\tau)$, $y(\tau)$ moves on the integral curves as indicated with the lapse of time τ and gets finally to the stable singular point.

In Fig. 2 we have three singularities, two of them, viz., (1) and (3) are stable and the correlated periodic oscillations are sustained. The another singularity (2) is a saddle point which is intrinsically unstable and the correlated periodic state can not last out, because any slight deviation from the point (2) will lead the oscillation to the stable state represented by either the point (1) or (3). It is also clear that one of the integral curves (the thick line in Fig. 2) which contains the saddle point (2) separates the plane into regions in one of which all integral curves tend to the singularity (1), and in the other region to the singularity (3).

Figure 4 shows these regions in r, θ-plane where r is the amplitude and θ is the phase angle of v at an instant at which the external force had been impressed, i. e.,

$$r=\sqrt{x^2(0)+y^2(0)}\,,\quad \theta=\arctan\frac{-y(0)}{x(0)}.$$

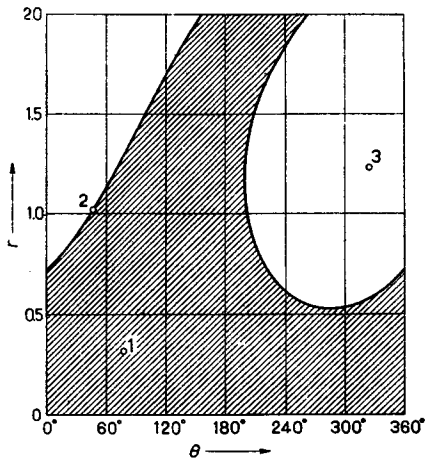

Fig. 4. Regions of initial conditions for the resonant oscillation (blank) and for the non-resonant oscillation (shaded).

One sees from Fig. 4 that an oscillation started with any initial conditions r and θ in the shaded region gets finally to the singularity (1), whereas an oscillation started from the remaining region gets to the singularity (3). One sees also that the singular point (2) is situated on the boundary of these two regions.

In Fig. 3 we have only one stable node, in other words, we have a single periodic solution for any initial conditions given.

It is obvious by Eqs. (2.3) that the amplitude and the phase angle of an oscillation in the neighborhood of the periodic state approach with time to that final state with damped sinusoids in case the corresponding singularity is a stable spiral, and approach to the final state with damped exponentials in case the singularity is a stable node. We can also see from Figs. 2 or 3 that the transient oscillation has higher frequency than that of the impressed force in case the initial condition r is comparatively large, because the point $x(\tau)$, $y(\tau)$ correlated with that

transient oscillation moves on a integral curve in the counter-clockwise direction around the origin 0.

4. Experimental Considerations

In this section we shall observe the nonlinear oscillations governed by the original equation (1.1) and compare the experimentally obtained result with the foregoing analysis.

The schematic diagram illustrated in Fig. 5 shows an electric circuit in which the nonlinear oscillations take place due to the saturable core inductance L under the alternating electromotive force $E\sin\omega t$. As noticed in the figure, the resistance R is shunted to the capacitance C to render the circuit dissipative. With the notations of Fig. 5, we have

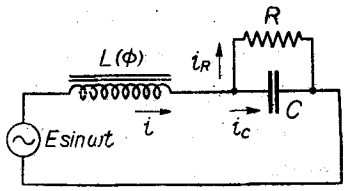

Fig. 5. Oscillatory circuit with nonlinear inductance.

$$\left.\begin{aligned} n\frac{d\phi}{dt} + Ri_R &= E\sin\omega t, \\ Ri_R &= \frac{1}{C}\int i_C\,dt, \\ i &= i_R + i_C, \end{aligned}\right\} \tag{4.1}$$

where n is the number of turns of the coil and ϕ denotes the magnetic flux in the core.

Let us now introduce dimensionless variables u and v in place of i and ϕ with the following relations:

$$i = I_n \cdot u, \quad \phi = \Phi_n \cdot v, \tag{4.2}$$

where I_n and Φ_n are appropriate unit quantities of the current and the flux respectively. Then, neglecting hysteresis, we may assume the saturation curve of the form:

$$u = c_1 v + c_3 v^3 + c_5 v^5 + \cdots\cdots, \tag{4.3}$$

where c_1, c_3, c_5, ... are constants characteristic to the core.

Although the units I_n and Φ_n can be chosen quite arbitrarily, it is preferable, for the brevity of calculation, to fix them with the following relations, i. e.,

$$\left.\begin{aligned} n\omega^2 C\Phi_n &= I_n, \\ c_1 + c_3 + c_5 + \cdots\cdots &= 1. \end{aligned}\right\} \tag{4.4}$$

Then, eliminating i_R and i_C in Eqs. (4.1) and substituting Eqs. (4.2), (4.3) and (4.4), we obtain

$$\left.\begin{aligned} &\frac{d^2v}{d\tau^2} + k\frac{dv}{d\tau} + c_1v + c_3v^3 + c_5v^5 + \cdots\cdots = B\cos\tau, \\ &\text{where} \\ &\tau = \omega t - \arctan k, \quad k = \frac{1}{\omega CR}, \\ &B = \frac{E}{n\omega\Phi_n}\sqrt{1+k^2}, \end{aligned}\right\} \qquad (4.5)$$

which is identical with the original equation (1. 1).

Now we proceed to show some experimental results which are effective to verify the foregoing analysis. As to the relation between the applied voltage E and the current i in Fig. 5, we have observed a good coincidence with the curves in Fig. 1, so that we have two stable periodic states under certain range of the applied voltage. We use to distinguish these two states as resonant and non-resonant according as the amplitude of the oscillation is larger or smaller. It is consequently clear that the singularity (3) in Fig. 2 is correlated with the resonant state and the singularity (1) is correlated with the non-resonant state.

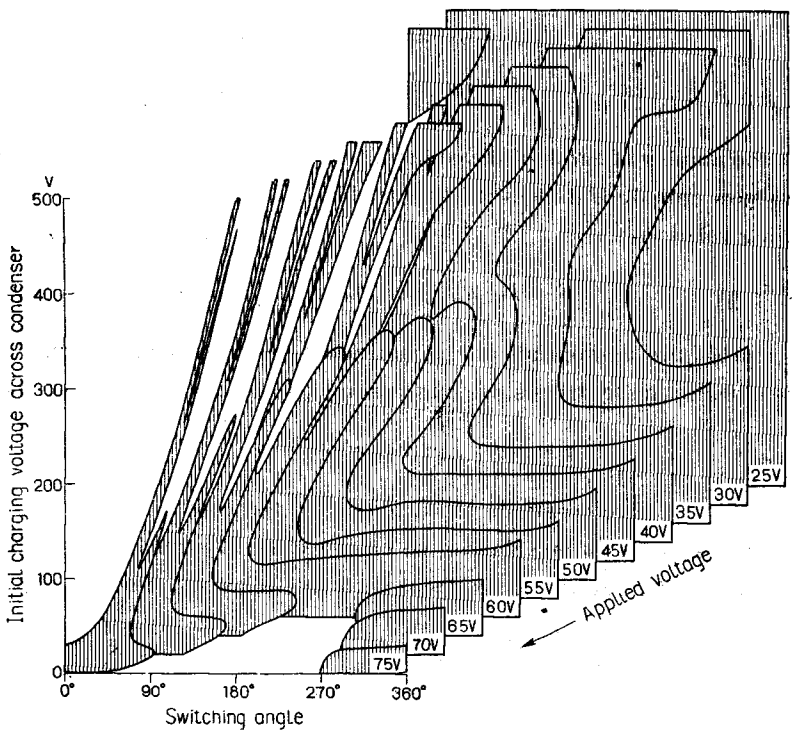

Fig. 6. Regions of initial conditions for the resonant oscillation (blank) and for the non-resonant oscillation (shaded) obtained under several values of the applied voltage.

In the foregoing analysis the initial conditions are prescribed with the rectangular components of $v(0)$, i. e., the coordinates $x(0)$, $y(0)$ of a point in the x, y-plane of Fig. 2. This is, however, not practical for our present experiment, so that we prescribed the initial conditions instead with the initial charging voltage across the condenser and the phase angle at the instant at which the voltage had been impressed on the circuit.[10]

Figure 6 shows the regions of initial conditions which lead either to the resonant state or the non-resonant state for several values of the applied voltage.[11] The shaded regions are for the non-resonant state, and, as may be expected, these regions are constricted with the increase of the applied voltage. These results are in accordance with the preceding analysis (cf. Fig. 4) except some slight discrepancies such as the branching of the shaded regions.

Part II. Subharmonic Oscillations

5. Analysis of the Subharmonic Oscillations by means of Integral Curves

Up to now we have considered the harmonic oscillations in which the frequency is the same as that of the external force. Permanent oscillations whose frequency is a fraction 1/2, 1/3, ..., $1/n$ of that of the impressed force can, however, occur in nonlinear systems, in particular in our case of the original equation (1. 1). To this phenomenon the term subharmonic oscillation is usually applied.

As a typical example of the subharmonic oscillations, we shall treat only one special case, i. e., the subharmonic oscillation of order 1/3 which is most frequently encountered in an oscillatory circuit containing saturable iron cores.[12]

We consider the differential equation

$$\frac{d^2v}{d\tau^2}+k\frac{dv}{d\tau}+v^3=B\cos 3\tau\,, \tag{5.1}$$

in which it is to be noticed that $3(\omega)$ represents the angular velocity of the impressed force $B\cos 3\tau$.

For the subharmonic oscillation of order 1/3, we may presume the form of the the solution of Eq. (5. 1) as:

10) In order to switch in the circuit at any desired phase angle of the applied voltage, we used an electronic switch consisted of two thyratrons connected in anti-parallel. The grids of these thyratrons are further controlled electronically to effect the accurate timing.

11) Before closing the circuit, the residual magnetism in the iron core has to be demagnetized or at least kept at a certain constant value in each measurement.

12) The subharmonic oscillations of other orders are similarly treated provided that the nonlinear characteristics are appropriately assumed.

$$v(\tau) = x(\tau)\sin\tau + y(\tau)\cos\tau + w\cos 3\tau\,. \tag{5.2}$$

Following Mandelstam and Papalexi,[13] the amplitude w of the component with the frequency of the external force is approximated by the following equation:

$$w = \frac{1}{1-3^2}B = -\frac{1}{8}B\,. \tag{5.3}$$

Substituting Eq. (5.2) into Eq. (5.1) and separately equating the terms containing $\sin\tau$ and $\cos\tau$ to zero, we obtain

$$\left.\begin{aligned} &\frac{dx}{d\tau} = \frac{1}{2}\left[-kx + Ay + \frac{3}{4}w(x^2-y^2)\right] \equiv X(x,y)\,,\\ &\frac{dy}{d\tau} = -\frac{1}{2}\left[Ax + ky + \frac{3}{4}w\cdot 2xy\right] \equiv Y(x,y)\,,\\ &\text{where}\\ &A = 1-\frac{3}{4}r^2 - \frac{3}{2}w^2\,,\quad r^2 = x^2+y^2\,. \end{aligned}\right\} \tag{5.4}$$

It is, however, to be remembered that the same restrictions with that mentioned in Section 1 have to be assumed for the derivation of Eqs. (5.4).

We can now proceed in the same way as for the harmonic oscillations. Hence the steady state oscillations are correlated with the singularities determined by

$$X(x, y) = 0\,,\quad Y(x, y) = 0\,, \tag{5.5}$$

and the transient solutions are discussed with the integral curves of the following equation:

$$\frac{dy}{dx} = \frac{Y(x, y)}{X(x, y)}, \tag{5.6}$$

where $X(x, y)$ and $Y(x, y)$ are given by Eqs. (5.4).

We now illustrate the integral curves of Eq. (5.6) for the following special case, i.e.,

$$k = 0.2\,,$$

$$B = 3.2 \quad [\text{accordingly } w = -0.4 \text{ by Eq. (5.3)}]\,,$$

and find the regions of initial conditions with which the final periodic solutions get to the subharmonic response.

The singularities correlated with the periodic solutions are determined by Eqs. (5.5) and summed up in the following table.

13) L. Mandelstam and N. Papalexi, Zeitschr. f. Phys., vol. 73, p. 227 (1931).

Singular point	x_0	y_0	$\lambda_{1,2}$	classification
Figure 7, (1)	−1.123	−0.378	$-0.100 \pm 0.599i$	stable spiral
ditto, (2)	0.889	−0.784	$-0.100 \pm 0.599i$	stable spiral
ditto, (3)	0.234	1.162	$-0.100 \pm 0.599i$	stable spiral
ditto, (4)	−0.858	0.209	0.365, −0.565	saddle (unstable)
ditto, (5)	0.610	0.639	0.365, −0.565	saddle (unstable)
ditto, (6)	0.248	−0.848	0.365, −0.565	saddle (unstable)
ditto, (7)	0	0	$-0.100 \pm 0.500i$	stable spiral

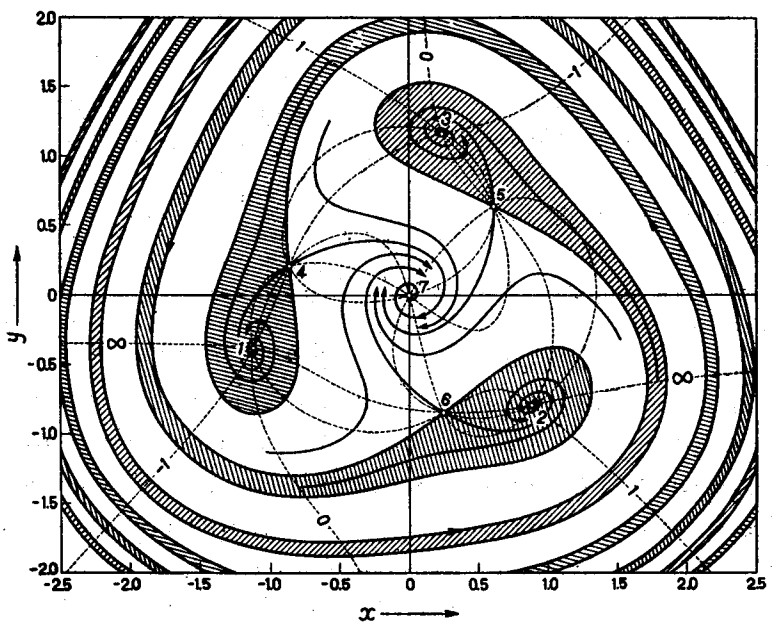

Full lines: integral curves Dotted lines: isoclines

Fig. 7. Integral curves for the subharmonic oscillation of order 1/3.

These singular points and the integral curves of Eq. (5.6) drawn with the aid of the isoclines are shown in Fig. 7. The singular points (1), (2), and (3) correlated with the subharmonic oscillations are equidistant from the origin $x=0$, $y=0$, and displaced to each other by 120° or one complete cycle of the impressed force. This is a plausible result for the subharmonic oscillation of order 1/3.

An oscillation started with the initial conditions in the shaded regions gets finally to the singularities (1), (2), or (3) correlated with the subharmonic response. Whereas any oscillation started from the remaining region gets to the singularity (7). Since $x=0$, $y=0$ at the singular point (7), no subharmonic oscillation takes place in this case.

Though it is omitted here, quite the same remarks as stated in Section 3 are also applied to the subharmonic oscillations.

6. Experimental Considerations

Referring again to the electric circuit containing the saturable iron core (cf. Fig. 5), we shall compare the foregoing analysis with experimental results.

We have first determined the region in which subharmonic oscillations of order 1/3 is stably maintained by varying the applied voltage V and the capacitance C of the oscillatory circuit. The experimental result is shown in Fig. 8 with the region shaded by hatched lines.

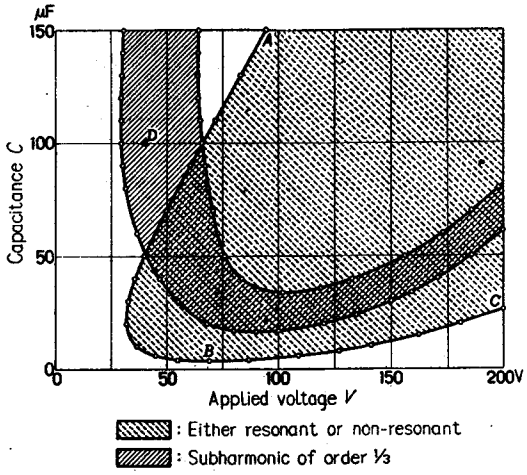

Fig. 8. Regions in which the oscillations of the different types sustain.

We have also determined the regions in which resonant and non-resonant harmonic oscillations may take place. The result is shown with the boundary ABC in Fig. 8. An oscillation which is first in the non-resonant state with a comparatively low voltage transfers into the resonant state when the voltage is raised up to the boundary BC. On the contrary, a transition takes place from the resonant to non-resonant state when the voltage is reduced down to the boundary AB (cf. Fig. 1). Hence in the interior of the boundary ABC shaded by dotted lines, either the resonant or non-resonant harmonic oscillations may take place according to the initial conditions given.

As a result of this, under the circumstances represented by a point D, viz.,

$$C = 100\mu\text{F}\ , \qquad V = 40\text{V}\ ,$$

we have two periodic states of oscillations, i.e., those of the non-resonant and subharmonic oscillations. Under these circumstances we have determined the regions of initial conditions which lead either to the non-resonant state or the subharmonic response. Figure 9 shows the experimental result. The shaded regions are for the subharmonic response and are in good accordance with the theoretical result of the preceding section (cf. Fig. 7).

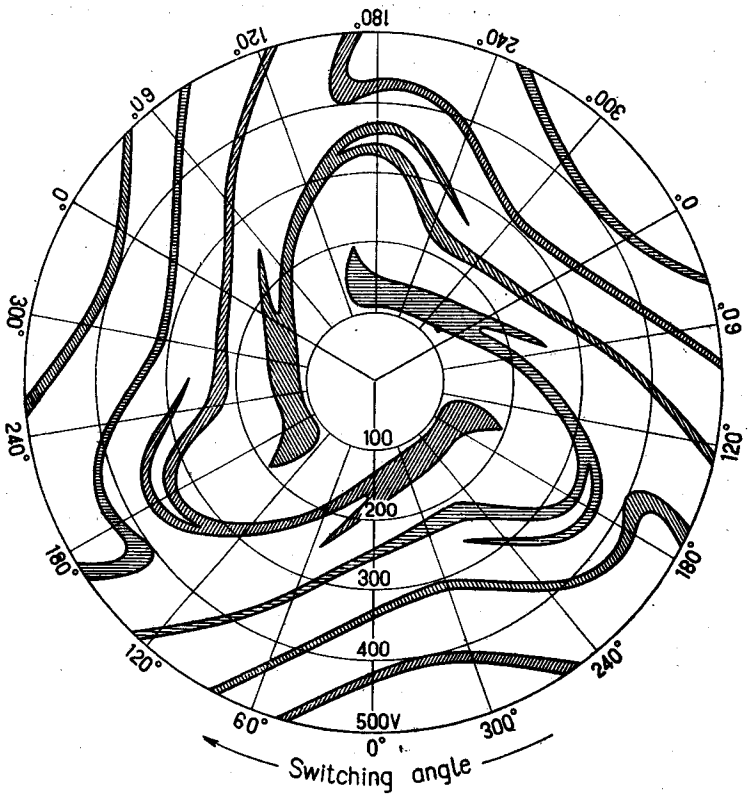

Radial scale: initial charging voltage across condenser

Fig. 9. Regions of initial conditions which lead to the subharmonic oscillation of order 1/3.

It is clear from Fig. 8 that the three kinds of periodic oscillations may sustain under certain circuit conditions.[14] Figure 10 is an experimental result obtained under such a condition. Although the theoretical analysis has not yet been accomplished, it may be expected by analogy with Figs. 6 and 9 that the regions of subharmonic oscillations are constricted by the apparition of the regions of resonant harmonic oscillations, and are distributed in narrower bands closely confined to each other.

7. Summary

Forced oscillations with nonlinear restoring force are studied in transient states as well as in steady states. The original differential equation characterized by a

14) These conditions are satisfied provided that the applied voltage and the capacitance are given within the region shaded by hatched lines and dots simultaneously.

nonlinear term is transformed under certain restrictions to the following differential equation of the first order:

$$\frac{dy}{dx}=\frac{Y(x,y)}{X(x,y)}.$$

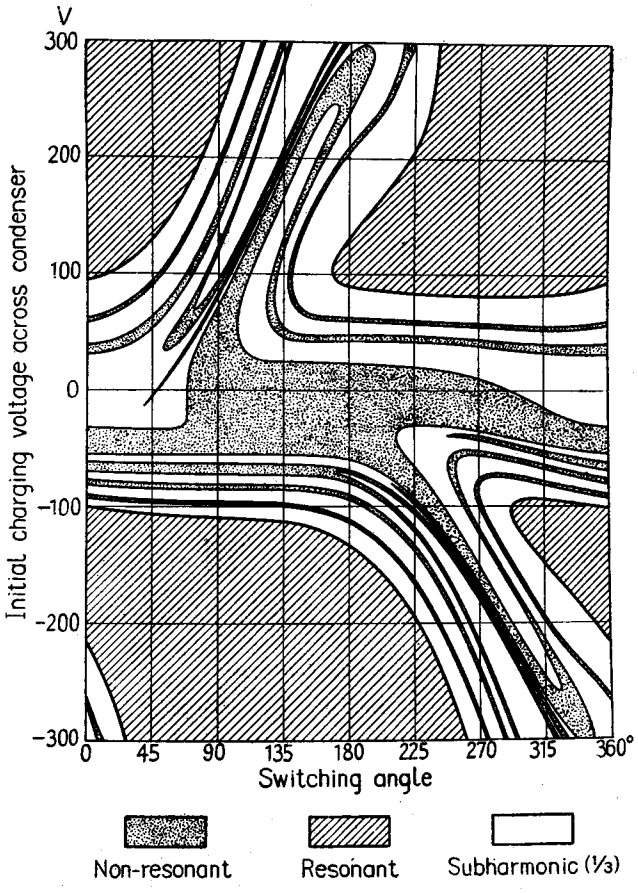

Fig. 10. Regions of initial conditions which lead to the different types of the periodic oscillations.

Following Poincaré and Bendixson, the singularities and the integral curves of the above equation are discussed, the former being correlated with the periodic states of oscillations and the latter with the transient states of oscillations. The stability of the periodic solutions is determined in accordance with that of the singular points, viz., according to the roots of the characteristic equation. The integral curves show the relationship between the given initial conditions and the periodic solutions. Thus, once the initial conditions are prescribed, we can foresee the final periodic states started with those conditions.[15]

With this method of investigation, we have studied the harmonic oscillations and the subharmonic oscillation of order 1/3.[16] In both cases the theoretical results are compared with the

15) As remarked at the end of the preceding section, this geometrical method of analysis fails for the case in which more than two states of periodic solutions may sustain in response to the different values of the initial conditions.

16) Some further investigations into the geometry of integral curves e. g., the limit cycle correlated with a quasi-periodic solution and Poincaré's "points singuliers de seconde espèce" correlated with periodic solutions under certain special cases) will be reported in the near future.

experimental observations obtained in an electric circuit containing a saturable iron core.

Acknowledgements

The help and encouragement given the author by Dr. R. Torikai in general, and by Drs. T. Matsumoto and S. Tomotika in particular, is gratefully acknowledged.

The starting point of this study was a paper published in 1943 by the same author in Jour. Inst. Elec. Eng. of Japan under the guidance of Dr. Torikai. In publishing this paper the author was fortunate in having the help of Dr. Tomotika.